Morphology of the ulnar insertion of the triangular fibrocartilage complex and related osseous landmarks

Masato Okuda,[a,*] Kotaro Sato MD,[a] Yoshikuni Mimata MD,[a] Kenya Murakami MD,[a] Gaku Takahashi MD,[b] Minoru Doita MD,[a]

[a] Department of Orthopaedic Surgery, Iwate Medical University, 2-1-1 Idaidori, Yahaba-cho, Shiwa-Gun, Iwate, Japan, 028-3695
[b] Department of Critical Care Medicine, Iwate Medical University, 2-1-1 Idaidori, Yahaba-cho, Shiwa-Gun, Iwate, Japan, 028-3695
MD, medical doctor

[*] **Corresponding author:**
Masato Okuda
TEL: 081 019-613-7111; Fax: 081 019-907-6996
E-mail: mstoct02@gmail.com
Department of Orthopaedic Surgery, Iwate Medical University, 2-1-1 Idaidori, Yahaba-cho, Shiwa-Gun, Iwate, Japan, 028-3695

Running head: ULNAR INSERTION OF THE TFCC

Keywords: Triangular Fibrocartilage Complex; TFCC; Foveal Tear; Morphology

Morphology of the ulnar insertion of the triangular fibrocartilage complex and related osseous landmarks

Abstract

Purpose: In triangular fibrocartilage complex (TFCC) injuries, a foveal tear of the radioulnar ligament (RUL) often requires surgery. Previous studies have suggested that surgeons should attach the TFCC to the center of the fovea because repaired eccentric fibers might tear or cause a loss of forearm rotation. The TFCC and its insertion points are small structures, and few studies have reported details of the foveal insertion. This study aimed to clarify the morphology of the ulnar insertion of the TFCC and related osseous landmarks with three-dimensional imaging.

Methods: This study used 26 formalin-fixed cadavers. At the ulna, the TFCC was inserted from the fovea to the middle part of the ulnar styloid. After gross observation of the TFCC, the ulnar insertion was outlined using a 1.0 mm drill. We then created three-dimensional images of the ulna using computed-tomography and marked (with software) an outline of the foveal insertion of the TFCC. We measured the area and the long and short diameters of the TFCC insertion.

Results: The area of the TFCC insertion was 34 mm^2 and positively correlated with the height of the ulnar styloid and the area of the ulnar head. The TFCC's highest point was 58% of the ulnar styloid height. The center of the TFCC insertion was 1.3 mm ulnar and 0.6 mm dorsal from the lowest point of the ulnar surface.

Conclusions: The center of the TFCC insertion was slightly ulnar of the lowest point of the ulnar surface. This study revealed the center, the area, and the osseous relation of the ulnar insertion of the TFCC.

Clinical relevance: When surgeons repair a TFCC foveal tear, they can find the anatomical center of the ulnar insertion efficiently and easily based on the osseous relationship.

Introduction

The triangular fibrocartilage complex (TFCC) is a fibrocartilage-ligament complex that spans the ulna, the radius, and the carpus.[1] The distal hammock-like structure and the dorsal and volar radioulnar ligament (RUL) comprise this complex.[1] The RUL arises from the radial sigmoid notch and inserts into the ulna in two separate sites.[2,3] The deep fiber inserts into the foveal region with an obtuse angle of attack, and the superficial fiber attaches around the ulnar styloid with an acute angle of attack.[2,3] In this anatomical feature, the deep component more effectively stabilizes the distal radioulnar joint (DRUJ) than the superficial component does throughout forearm rotation.[2,3]

The TFCC is a biomechanically effective intrinsic radioulnar component and is the primary stabilizer of the DRUJ.[2-4] Other extrinsic stabilizers are the extensor carpi ulnaris tendon and tendon sheath, pronator quadratus, bone, capsule, and interosseous membrane.[2-4] Anatomical and biomechanical studies revealed the function of the RUL during pronation-supination.[2-4] A previous report revealed that in forearm pronation, dorsal superficial fibers of the RUL must be tightened for stability, as do the deep volar fibers of the RUL. Conversely, in supination, the palmar superficial fiber of the RUL should be tightened, as do the deep dorsal fibers of the RUL.[2,5] An RUL tear at the ulnar insertion causes ulnar-side pain or DRUJ instability and often requires surgery.[6-9] Although previous studies revealed the morphology and biomechanics of the TFCC, detailed information about foveal attachment is not clear.[10-13] Even using high-resolution magnetic resonance imaging, visualization of this small insertion is challenging.[14-16]

This study aimed to clarify the accurate point of foveal insertion of the TFCC, and related osseous landmarks with three-dimensional (3D) computed tomography imaging. This method is useful for measuring the distance and area of insertion at the unevenly shaped ulnar head.[10]

Materials and Methods

The ethics committee at our institution approved this study (No.MH2018-075). A sample of convenience comprising 35 cadaveric left-upper limbs (18 from males and 17 from females) were dissected. These cadavers were donated to our institute for education and research purposes. The mean age at the time of death was 81 (range, 67 to 97) years. All specimens had been fixed with 10% formalin and preserved in 50% alcohol for 6 months according to our institution's protocol. Of the 35 specimens, eight specimens with severe macroscopic changes and one limb with an ulnar insertion tear of the TFCC were excluded. Thus, 26 limbs (14 males and 12 females) remained for this study. The mean width of the ulnar head (volar-dorsal length) was 19 mm and 16 mm for the males and females, respectively. The mean width of the ulnar head (radial-ulnar length) was 18 mm and 16 mm for the males and females, respectively. Among these, 15 specimens had a damaged disc.

The limbs used in this study were amputated in the middle part of the forearm. Dissection began by removing the skin and subcutaneous tissue on the forearm, and flexor and extensor tendons. Next, we detached the wrist joint capsule from the carpal bones, removed the carpal bones, and exposed the joint surface of the radius and ulna. After carefully separating the wrist joint capsule from the TFCC, we could see the outlines of the TFCC. We were able to distinguish the TFCC fiber from the capsule, as it was a nonligamentous soft tissue. We subsequently detached the TFCC from the radius to expose the ulnar insertion (Fig. 1). After gross observation, we outlined the ulnar insertion of the TFCC using a 1.0 mm drill (Fig. 2).

Three-dimensional visualization

The ulna was scanned using a 16-row multi-slice computed tomography scanner (ECLOS; Hitachi Medical Corporation, Tokyo, Japan) and all digital imaging data were transferred to a dedicated software (Mimics version 19.0; Materialise N.V., Belgium) to create 3D images of the ulna. After creating the 3D images, the ulnar insertion of the TFCC and its related osseous landmarks were measured. All analyses were performed with the 3D images.

Determination of the TFCC insertion in the horizontal plane

In the horizontal plane, we drew a circle on the outline of the ulnar head and then set the ulnar styloid on the X-axis (Fig. 3). The center of the circle was defined as point O. The first author marked the TFCC insertion area according to the drill hole (Fig. 3). The software defined the center of the TFCC insertion as point T. The lowest point of the ulnar surface in the 3D view was defined as point L, which is an easily recognized osseous landmark on the surface of the ulna. We measured the linear distance between point O and point T and between point T and point L.

Measurements of the TFCC insertion in the horizontal plane

The area of the TFCC insertion was marked according to the drill hole and measured using software. The first author measured the long and short diameters of the TFCC insertion and the area of the ulnar head in that plane (Fig. 3). Finally, the first author examined the correlation between the area of the TFCC insertion and the area of the ulnar head.

Measurements of the TFCC insertion in the coronal plane

In the coronal plane, we marked the apex of the ulnar styloid, the highest point of TFCC insertion of the ulnar styloid, and the lowest point of the ulnar surface (point L) (Fig. 4). We defined the height from point L to the apex of the ulnar styloid as the height of the ulnar styloid. Then, the height from point L to the highest point of the TFCC insertion to the ulnar styloid was measured. Finally, we examined the correlation between the area of the TFCC insertion and the height of the ulnar styloid.

The first author measured the parameters and used the mean of the two measurements as the final value. The accuracy of the 3D models generated by the computed tomography data had a mean error of 0.2 ± 0.31 mm (mean ± standard deviation) or about one-third of the pixel size.[17] The correlation was analyzed using Pearson's correlation coefficient test, and $P<0.05$ was considered statistically significant.

Results

Location of the center of the TFCC insertion

In the horizontal plane, point T was 4.1 ± 1.1 mm (range, 6.7 to 2.1) ulnar and 0.1 ± 0.6 mm (range, -1.1 to 1.3) dorsal from point O. Point T was 1.3 ± 0.9 mm (range, 3.2 to -0.57) ulnar and 0.6 ± 0.9 mm (range, 1.7 to -1.4) dorsal from point L. Point L was 2.8 ± 1.4 mm (range, 6.0 to 0.5) ulnar and 0.6 ± 1.2 mm (range, 2.7 to -1.9) palmar from point O (Fig. 5).

Measurements of the TFCC insertion

The area of the TFCC insertion was 34 ± 22 mm^2. The area of the ulnar head was 230 ± 51 mm^2. The long diameter of the TFCC insertion was 9 ± 2 mm and the short diameter of the TFCC insertion was 6 ± 1 mm (Figs. 3, 6, 7). The area of the TFCC insertion positively correlated with the area of the ulnar head ($R=0.70$, $P<0.05$) (Fig. 8).

Relationship of the TFCC insertion and ulnar styloid

In the coronal plane, the ulnar styloid height was 5 ± 1 mm. The highest point of the TFCC was 3 ± 1 mm (58% of the ulnar styloid height). The area of the TFCC insertion positively correlated with the height of the ulnar styloid ($R=0.57$, $P<0.05$) (Fig. 9).

Discussion

This study revealed the location of the center of the TFCC insertion as being slightly ulnar from the lowest point of the ulnar surface. We were unable to distinguish the RUL into the proximal and deep component macroscopically. Shin et al. independently identified deep and superficial components in a cadaver study using dissecting microscope.[10] In their study, the average distance between the fovea center and ulnar head center was 2.4mm. Point L identified in our study is close to their fovea center. They mentioned that loose connective tissue filled the insertion site between the deep and superficial fibers. In our study, we reserved this tissue because it was difficult to separate in the macroscopic dissection. Our findings would be regarded as outline of the insertion of both the deep and superficial components described by Shin et al.[10] Biomechanical studies reported that the deep component provides more stability than the superficial component and that the foveal origin was more important.[2,3,18] Kataoka et al. demonstrated the pronosupination center of the ulnar head in 3D images.[19] They described the ulnar head in the horizontal plane as a circle similar to our 3D image. In their report, the pronosupination center was located approximately 2.6 mm ulnar and slightly palmar from the center of the ulnar head.[19] Based on a comparison of their data and our results, point L identified in our study is close to the above mentioned pronosupination center. As point T consists of both deep and superficial insertions, the center of the deep component of the RUL would be more radial than point T. We reckon that point L can act as the center of the deep component of the RUL to which surgeons should attach the TFCC. Further biomechanical studies are necessary in relation to this concept.

In the present study, the ulnar insertion area of the RUL was approximately 34 mm^2 and it was inserted into the fovea at approximately 58% of the height of the ulnar styloid. The DRUJ has both rotational and translational movements.[4,19,20] In supination, the ulna is located palmar relative to the radius, and in pronation, it is more dorsal.[4,19,20] Tay et al. conducted an in-vivo kinematic analysis of forearm rotation.[21] They showed that the axis at the DRUJ varied depending on the forearm. The relatively large TFCC insertion area in our study is consistent with those findings. This suggests that depending on the forearm position, different parts of the RUL fibers are responsible for the in-vivo variability of the forearm axis. Currently, several surgical methods for ulnar insertion injury of the TFCC have been reported and reattachment to the fovea is the principal strategy.[7-9,22-24] Few studies discuss the size of the attachment area. Iwasaki created a 2.9 mm osseous tunnel at the fovea, indicating a 2.9 mm diameter attachment area in their method.[9] Further, the ulnar RUL insertion area showed a positive correlation with the area of the ulnar head and the height of the ulnar styloid. Our results showed an ulnar RUL insertion mean of 9 mm as the long and 6 mm as the short diameter. Although a greater attachment area may stabilize both, the proximal and distal components, it could cause a loss of forearm rotation. Biomechanical and clinical studies are needed to clarify the optimal size of the foveal attachment.

In previous reports regarding TFCC repair, surgeons were unable to distinguish the superficial and deep components.[7-9,22-24] In the future, with the development of new and improved surgical instruments and techniques, surgeons will be able to reattach the deep component of the RUL and superficial component independently. In the future, surgeons trying to reproduce the superficial component may need to work more towards the ulnar side than the anatomical center. Additional studies are necessary to elucidate this potential challenge.

In this study, the center of the ulnar insertion was 1.3 mm ulnar and 0.6 mm dorsal from the lowest point of the fovea. The osseous relationship might be a good landmark during surgery. There are several ways to target and identify an attachment point, such as direct vision, palpation, C-arm X-ray, and targeting devices.[9,22] When skilled, knowledgeable surgeons use targeting devices or palpation, they usually find the lowest point of the fovea and the anatomical center of the RUL insertion quickly and easily.

This study has several limitations. First, the mean age of the cadavers was 81 years. Although we excluded severe macroscopic changes and an ulnar insertion tear of the TFCC, 15 specimens had a damaged disc. It might affect degeneration of the ulnar insertion of the TFCC. Deformity or spur formation of the ulnar head might have affected the identification of the TFCC and osseous landmarks. Second, we used formalin-fixed specimens. Embalmed specimens cannot adequately represent in vivo conditions and might have affected the dissection of the TFCC and soft tissues. Third, this study used an accurate method of 3D measurement and visualization, however this technique involved human dissection and subjective decisions regarding the TFCC insertion, which may have led to error and bias. We used a 1.0 mm drill for outlining the TFCC, and this could have affected the measurements. However, the software was unable to clearly visualize a hole less than 1.0 mm. Fourth, we investigated the ulnar insertion of the RUL: however, the anatomical relationships between the TFCC and the surrounding soft tissues are also important. We were unable to explore the soft tissue relationship in this study. Finally, we did not investigate the isometric point of the RUL insertion or stability of the DRUJ. Although we clarified the anatomical point of attachment, we are uncertain as to whether it is clinically optimal. A biomechanical study is necessary to validate the clinical application of this study.

References

1. Nakamura T, Takayama S, Horiuchi Y, Yabe Y. Origins and insertions of the triangular fibrocartilage complex: a histological study. J Hand Surg Br. 2001;26:446-454.

2. Kleinman WB. Stability of the distal radioulna joint: biomechanics, pathophysiology, physical diagnosis, and restoration of function what we have learned in 25 years.J Hand Surg Am. 2007;32:1086-1106.

3. Haugstvedt JR, Langer MF, Berger RA. Distal radioulnar joint: functional anatomy, including pathomechanics. J Hand Surg Eur. 2017;42:338-345.

4. Stuart PR, Berger RA, Linscheid RL, An KN. The dorsopalmar stability of the distal radioulnar joint. J Hand Surg Am. 2000;25:689-699.

5. Xu J, Tang JB. In vivo changes in lengths of the ligaments stabilizing the distal radioulnar joint. J Hand Surg Am. 2009;34:40-45.

6. Atzei A, Luchetti R. Foveal TFCC tear classification and treatment. Hand Clin. 2011;27:263-272.

7. Park JH, Kim D, Park JW. Arthroscopic one-tunnel transosseous foveal repair for triangular fibrocartilage complex (TFCC) peripheral tear. Arch Orthop Trauma Surg. 2018;138:131-138.

8. Shinohara T, Tatebe M, Okui N, Yamamoto M, Kurimoto S, Hirata H. Arthroscopically assisted repair of triangular fibrocartilage complex foveal tears. J Hand Surg Am. 2013;38:271-277.

9. Iwasaki N, Minami A. Arthroscopically assisted reattachment of avulsed triangular fibrocartilage complex to the fovea of the ulnar head. J Hand Surg Am. 2009;34:1323-1326.

10. Shin WJ, Kim JP, Yang HM, Lee EY, Go JH, Heo K. Topographical Anatomy of the Distal Ulna Attachment of the Radioulnar Ligament. J Hand Surg Am. 2017;42:517-524.

11. Matsumoto T, Tang P, Fujio K, Strauch RJ, Rosenwasser MP. The optimal suture placement and bone tunnels for TFCC repair: a cadaveric study. J Wrist Surg. 2018;7:375-381.

12. Makita A, Nakamura T, Takayama S, Toyama Y. The shape of the triangular fibrocartilage during pronation-supination. J Hand Surg Br. 2003;28:537-545.

13. Kataoka T, Moritomo H, Omokawa S, Iida A, Wada T, Aoki M. Palmar reconstruction of the triangular fibrocartilage complex for instability of the distal radioulnar joint: a biomechanical study. J Hand Surg Eur Vol. 2013;38:515-522.

14. Tanaka T, Yoshioka H, Ueno T, Shindo M, Ochiai N. Comparison between high-resolution MRI with a microscopy coil and arthroscopy in

triangular fibrocartilage complex injury. J Hand Surg Am. 2006;31:1308-1314.

15. von Borstel D, Wang M, Small K, Nozaki T, Yoshioka H. High-Resolution 3T MR Imaging of the Triangular Fibrocartilage Complex. Magn Reson Med Sci. 2017;16:3-15.

16. Nozaki T, Rafijah G, Yang L, et al. High-resolution 3 T MRI of traumatic and degenerative triangular fibrocartilage complex (TFCC) abnormalities using Palmer and Outerbridge classifications. Clin Radiol. 2017;72:904.e1-904.e10.

17. Gelaude F, Vander Sloten J, Lauwers B. Accuracy assessment of CT-based outer surface femur meshes. Comput Aided Surg. 2008;13:188-199.

18. Haugstvedt JR, Berger RA, Nakamura T, Neale P, Berglund L, An KN. Relative contributions of the ulnar attachments of the triangular fibrocartilage complex to the dynamic stability of the distal radioulnar joint. J Hand Surg Am. 2006;31:445-451.

19. Kataoka T, Moritomo H, Omokawa S, Iida A, Murase T, Sugamoto K. Ulnar variance: its relationship to ulnar foveal morphology and forearm kinematics. J Hand Surg Am. 2012; 37:729-735.

20. King GJ, McMurtry RY, Rubenstein JD, Gertzbein SD. Kinematics of the distal radioulnar joint. J Hand Surg Am. 1986;11:798-804.

21. Tay SC, van Riet R, Kazunari T, Amrami KK, An KN, Berger RA. In-vivo kinematic analysis of forearm rotation using helical axis analysis. Clin Biomech (Bristol, Avon). 2010;25:655-659.

22. Nakamura T, Sato K, Okazaki M, Toyama Y, Ikegami H. Repair of foveal detachment of the triangular fibrocartilage complex: open and arthroscopic transosseous techniques. Hand Clin. 2011;27:281-290.

23. Yao J. All-arthroscopic triangular fibrocartilage complex repair: safety and biomechanical comparison with a traditional outside-in technique in cadavers. J Hand Surg Am. 2009;34:671-676.

24. Atzei A. New trends in arthroscopic management of type 1-B TFCC injuries with DRUJ instability. J Hand Surg Eur Vol. 2009;34:582-591.

Figure Legends

Fig. 1 Dissected ulnar head and TFCC of the left wrist. The TFCC inserts from the fovea to the middle part of the ulnar styloid.

Fig. 2 The ulnar insertion of the TFCC is outlined using a 1.0 mm drill.

Fig. 3 Horizontal plane of the ulnar head. The arrow heads indicate the drill holes. The red dot indicates the center of the circle formed by the ulnar head (point O). The yellow dot indicates the center of the TFCC insertion (point T), and the blue dot indicates the lowest point of the fovea (point L). The red area shows the insertion area of the TFCC.

Fig. 4 Coronal plane of the ulnar head (palmar view). The orange dot, black dot, and blue dot indicate the apex of the ulnar styloid, the highest point of the TFCC insertion, and the lowest point of the ulnar surface, respectively. The yellow dot indicates the center of the TFCC insertion. The large arrow and small arrow indicate the height of the ulnar styloid and height of the TFCC insertion, respectively.

Fig. 5 In the original coordinate plane in the horizontal view of the ulnar head, the origin of the coordinates is at the center of the circle formed by the ulnar head. The ulnar styloid is on the X-axis. Yellow dots plot the centers of the TFCC, and the large yellow dot indicates the mean position. The blue dots indicate the lowest point of the ulnar surface, and the large blue dot indicates the mean position.

Fig. 6 Dorsal view of the ulnar head.

Fig. 7 Multidirectional view of the ulnar head.

Fig. 8 The TFCC insertion area is positively correlated with the area of the ulnar head ($R = 0.70$, $P < 0.05$).

TFCC: triangular fibrocartilage complex

Fig. 9 The TFCC insertion area is positively correlated with the height of the ulnar styloid ($R=0.57$, $P<0.05$).

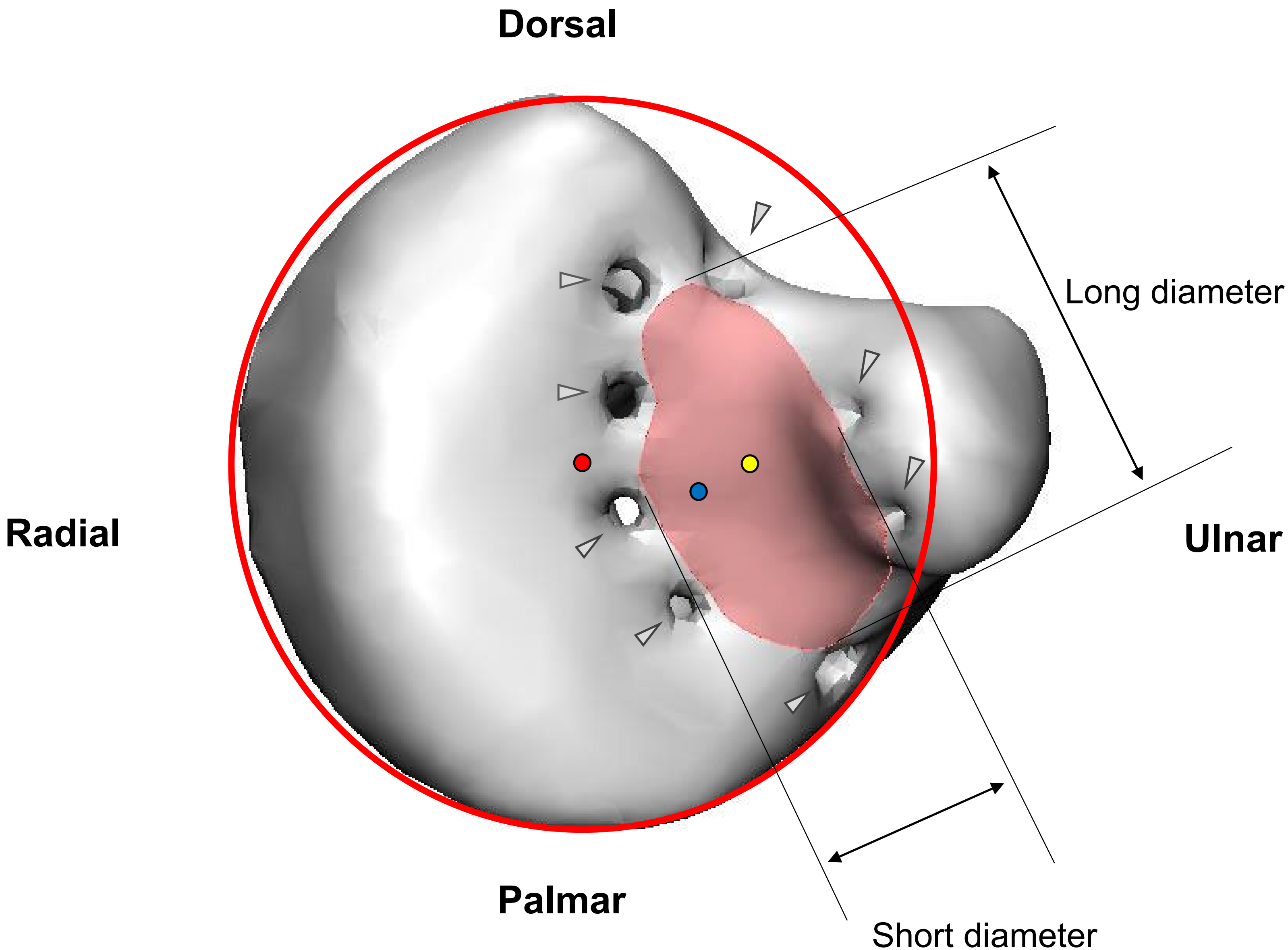
Dorsal
Long diameter
Radial
Ulnar
Short diameter
Palmar

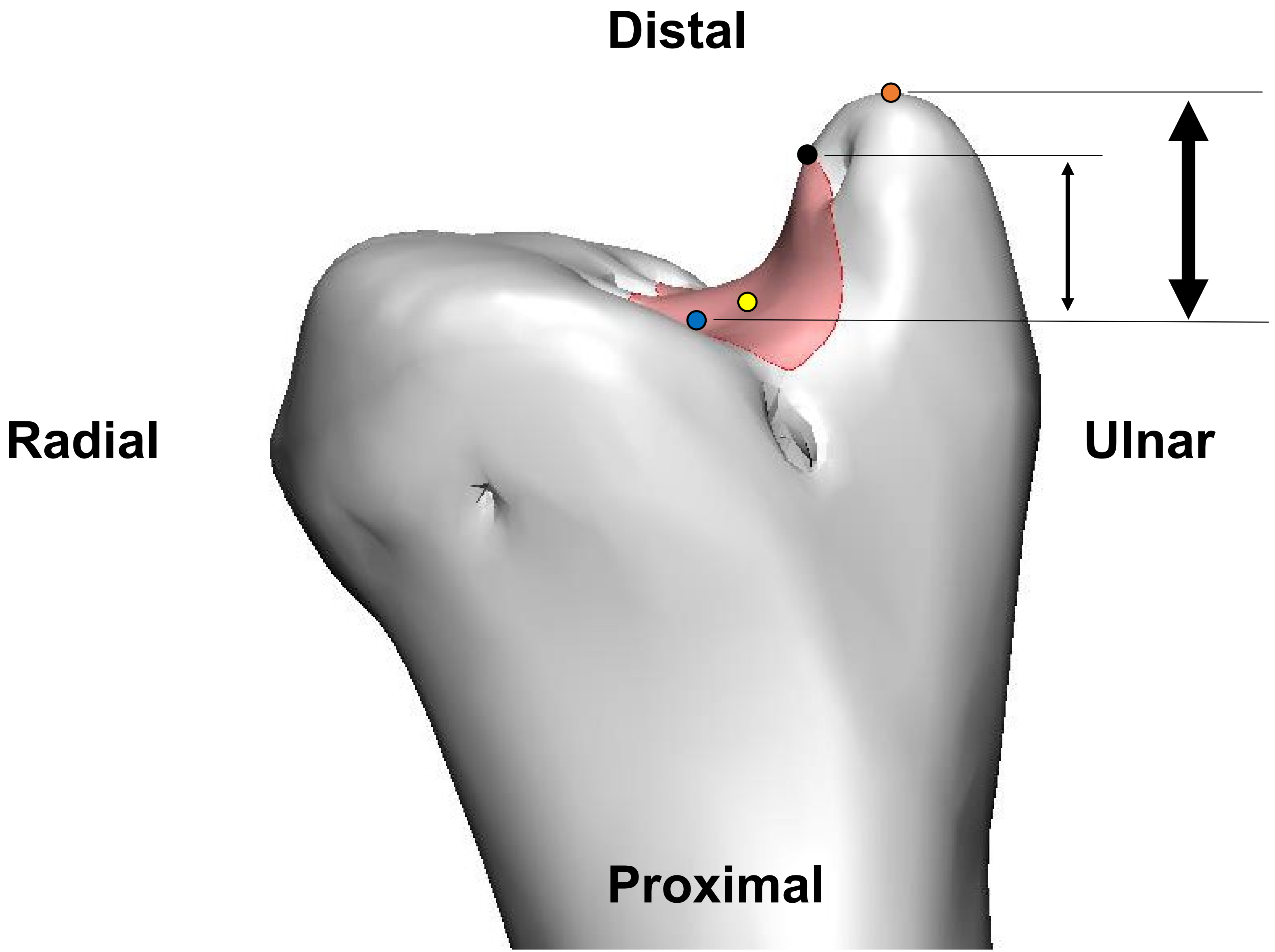

Distal
Radial
Ulnar
Proximal

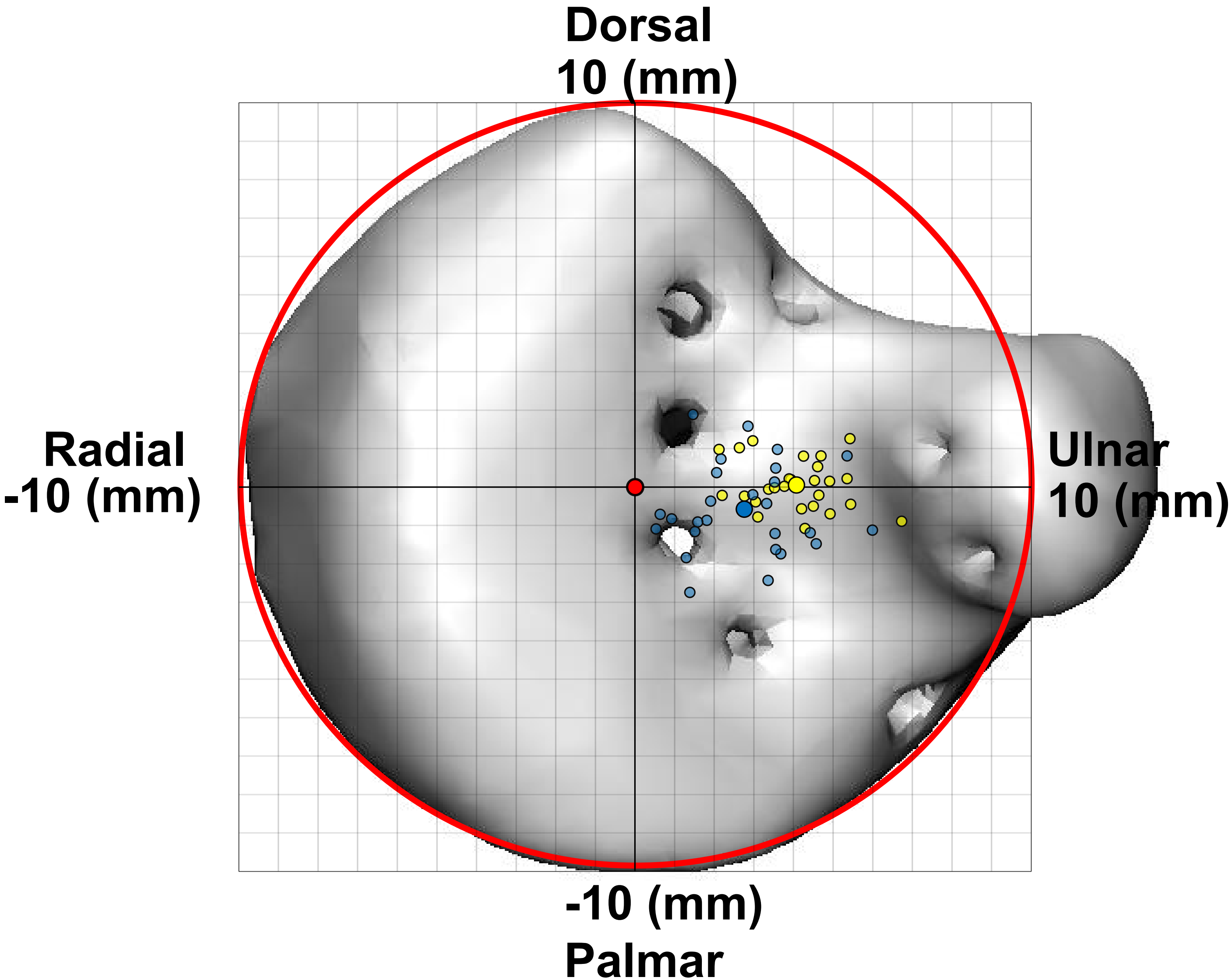
Dorsal
10 (mm)
Radial
-10 (mm)
Ulnar
10 (mm)
-10 (mm)
Palmar

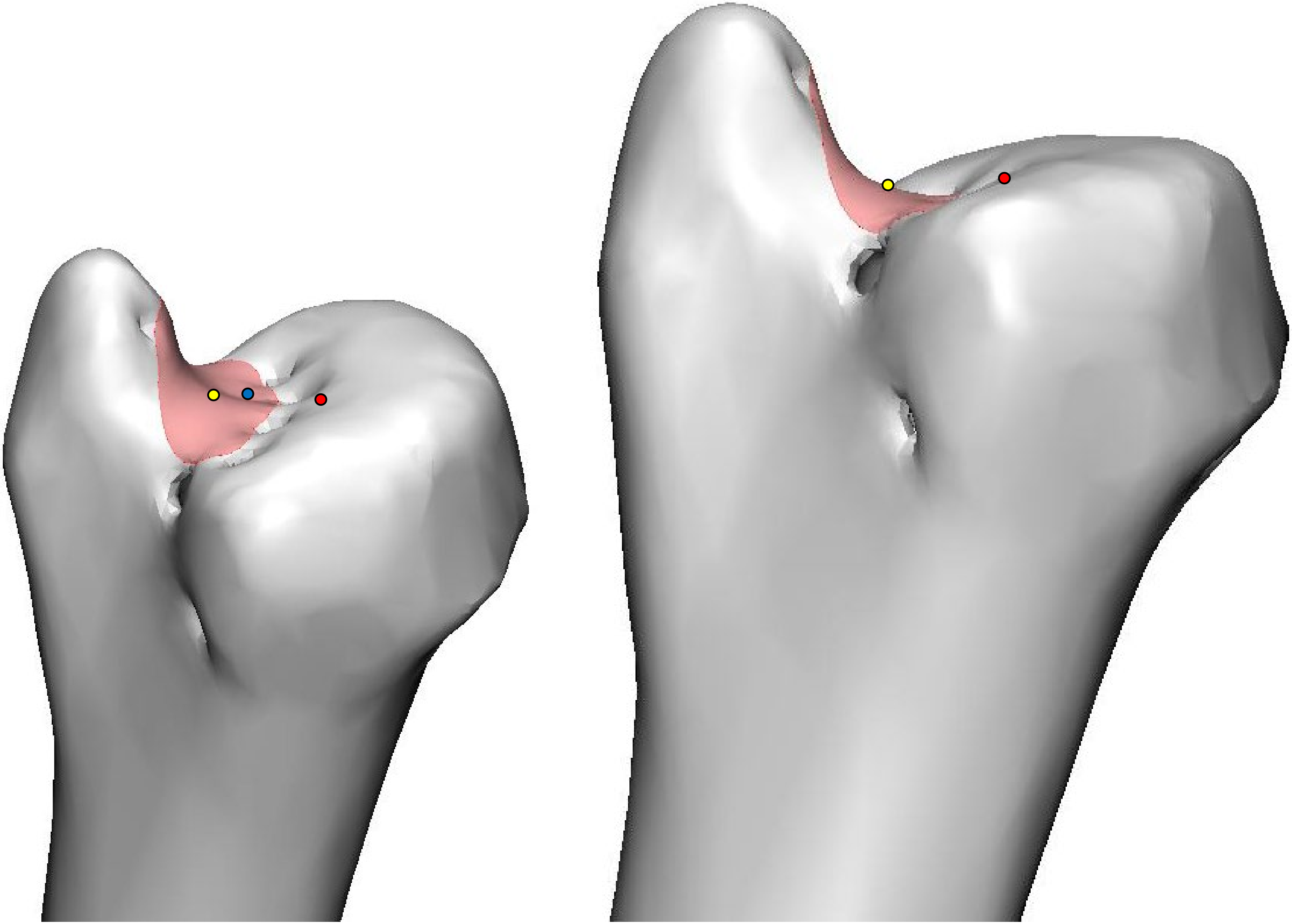

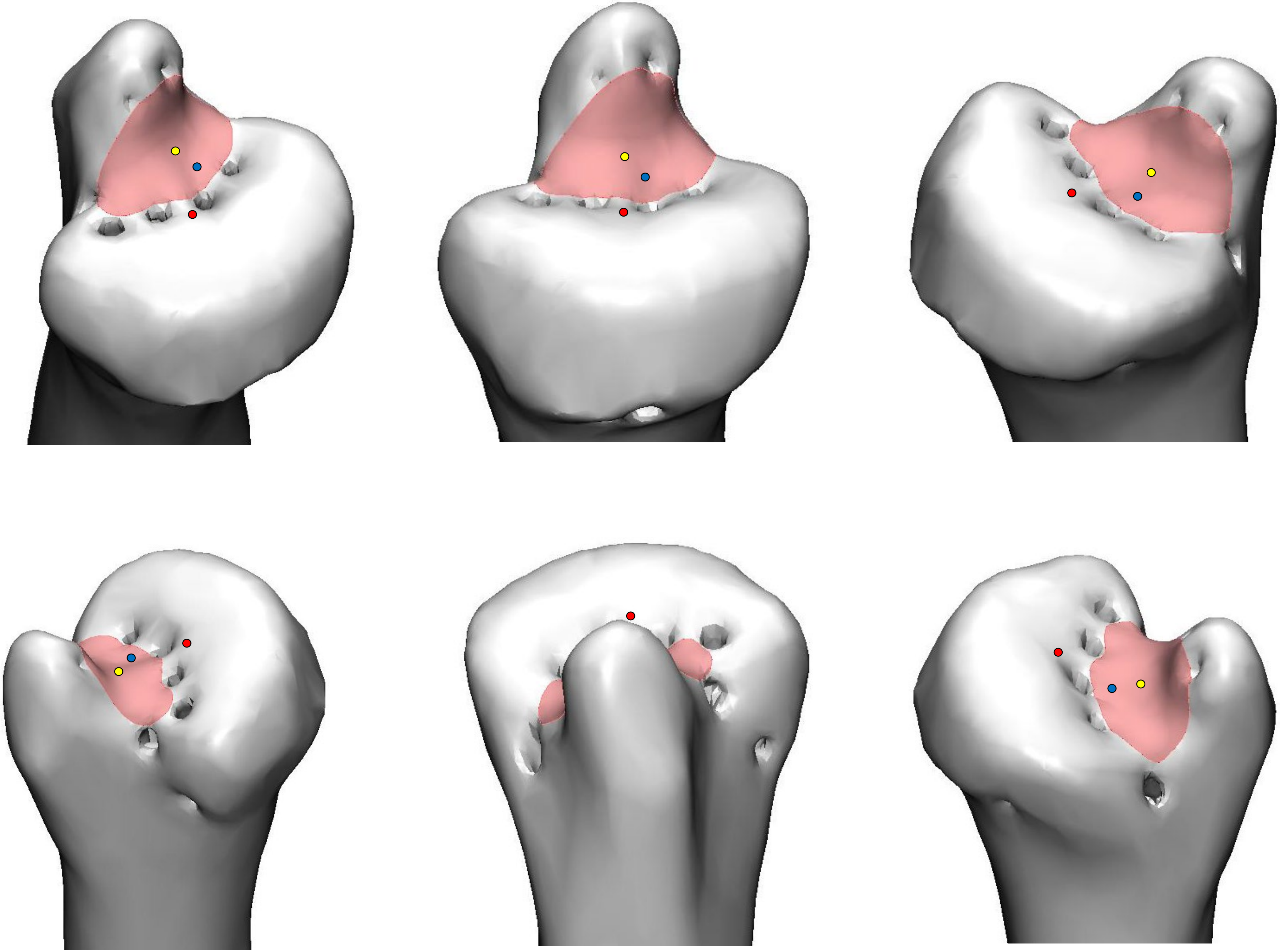

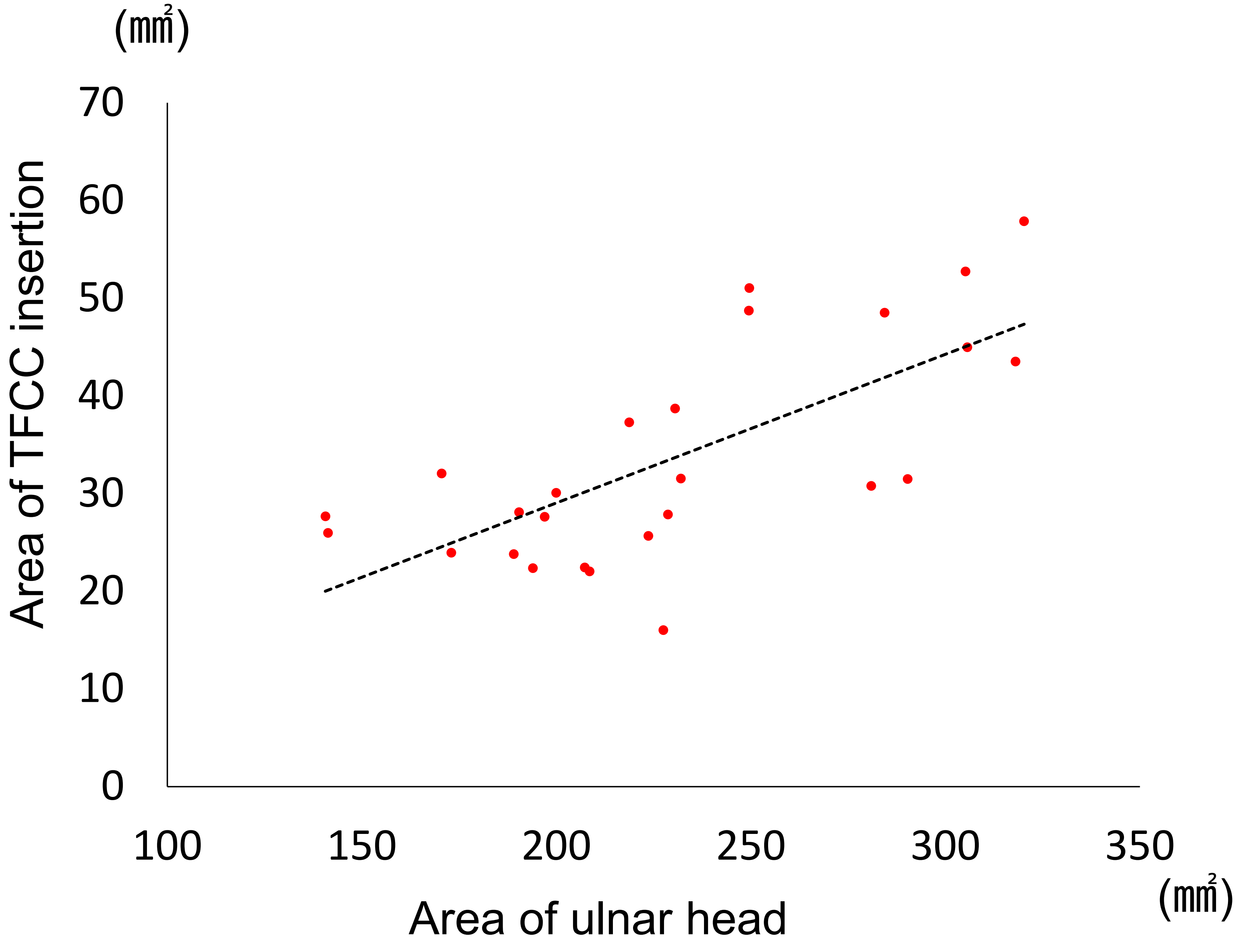

(㎟)
70
60
50
40
30
20
10
0
Area of TFCC insertion
100
150
200
250
300
350
(㎟)
Area of ulnar head

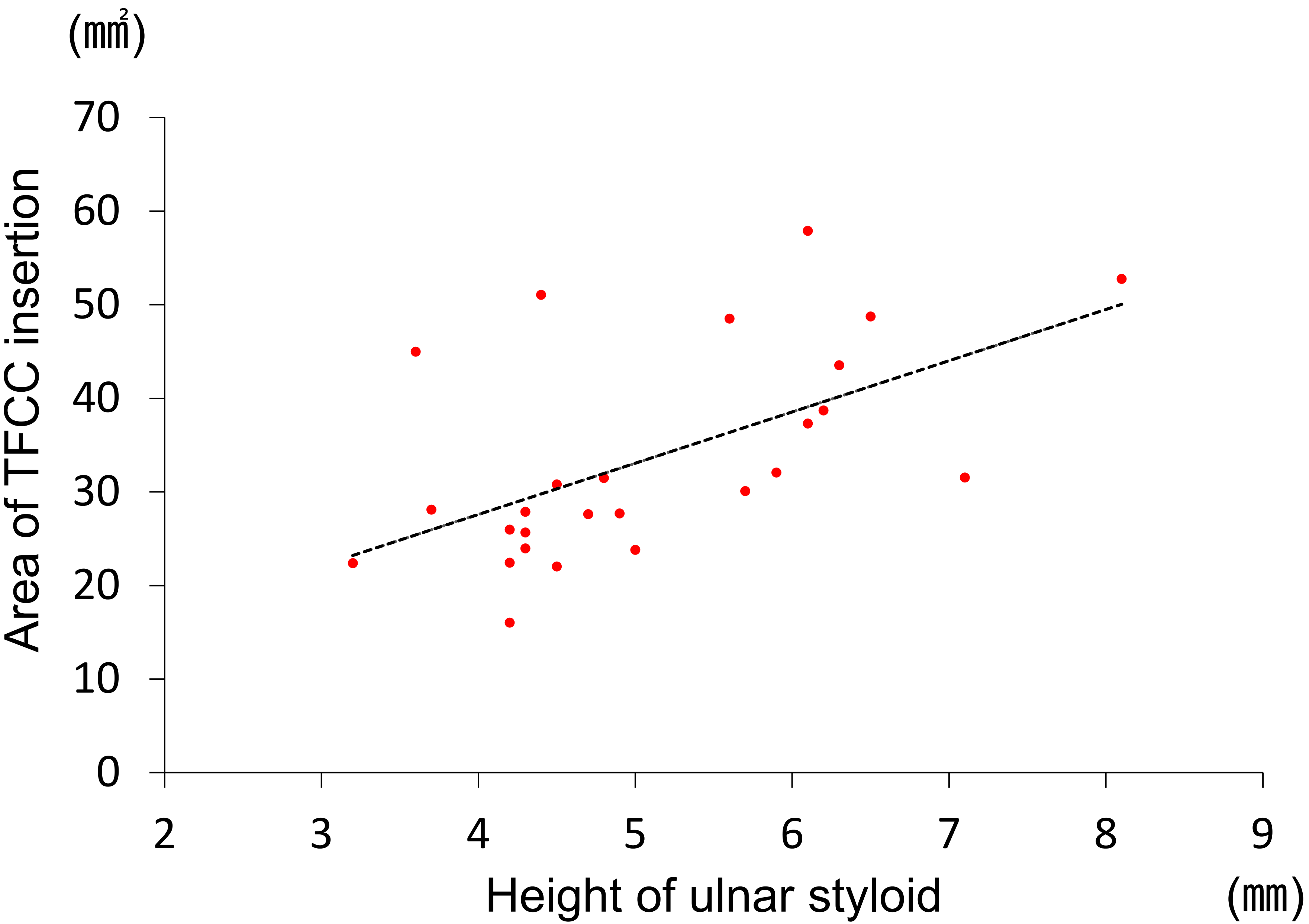

(㎟)
70
60
50
40
30
20
10
0
Area of TFCC insertion
2
3
4
5
6
7
8
9
Height of ulnar styloid
(㎜)